earth

Article

Spatio-Temporal Evolution of Rainfall over the Period 1981–2020 and Management of Surface Water Resources in the Nakanbe–Wayen Watershed in Burkina Faso

Wennepinguere Virginie Marie Yameogo [1,2,*], You Lucette Akpa [3], Jean Homian Danumah [3], Farid Traore [2], Boalidioa Tankoano [1], Zezouma Sanon [2], Oumar Kabore [2] and Mipro Hien [1]

1 Département Environnement, Eaux et Forêts, Université Nazi BONI (UNB), Bobo–Dioulasso P.O. Box 1091, Burkina Faso; boalidioa.tankoano@u-naziboni.net (B.T.); mipro.hien@u-naziboni.net (M.H.)
2 Département Gestion des Ressources Naturelles, Institut de l'Environnement et de Recherches Agricoles (INERA), Ouagadougou P.O. Box 8645, Burkina Faso; farid.traore@cnrst.gov.bf (F.T.); zezouma.sanon@cnrst.gov.bf (Z.S.); oumar.kabore@cnrst.gov.bf (O.K.)
3 Centre Universitaire de Recherche et d'Application en Télédétection (CURAT), UFR-STRM, Université Félix Houphouët Boigny, Abidjan P.O. Box 801, Côte d'Ivoire; lucette.akpa@curat-edu.org (Y.L.A.); jeanh.danumah@curat-edu.org (J.H.D.)
* Correspondence: wennepinguere.virginie@cnrst.gov.bf; Tel.: +226-70295994 or +226-54650202

Abstract: Spatio-temporal analysis of rainfall trends in a watershed is an effective tool for sustainable water resources management, as it allows for an understanding of the impacts of these changes at the watershed scale. The objective of the present study is to analyze the impacts of climate change on the availability of surface water resources in the Nakanbe–Wayen watershed over the period from 1981 to 2020. The analysis was conducted on in situ rainfall data collected from 14 meteorological stations distributed throughout the watershed and completed with CHIRPS data. Ten precipitation indices, recommended by the ETCCDI (Expert Team on Climate Change Detection and Indices), were calculated using the RClimDex package. The results show changes in the distribution of annual precipitation and an increasing trend in annual precipitation. At the same time, a trend towards an increase in the occurrence and intensity of extreme events was also observed over the last 4 decades. In light of these analyses, it should be emphasized that the increase in precipitation observed in the Nakanbe–Wayen watershed is induced by the increase in the occurrence and intensity of events, as a trend towards an increase in persistent drought periods (CDD) is observed. This indicates that the watershed is suffering from water scarcity. Water stress and water-related hazards have a major impact on communities and ecosystems. In these conditions of vulnerability, the development of risk-management strategies related to water resources is necessary, especially at the local scale. This should be formulated in light of observed and projected climate extremes in order to propose an appropriate and anticipated management strategy for climate risks related to water resources at the watershed scale.

Keywords: climate change; RclimDex; precipitation; extreme indices; trend analysis

Citation: Yameogo, W.V.M.; Akpa, Y.L.; Danumah, J.H.; Traore, F.; Tankoano, B.; Sanon, Z.; Kabore, O.; Hien, M. Spatio-Temporal Evolution of Rainfall over the Period 1981–2020 and Management of Surface Water Resources in the Nakanbe–Wayen Watershed in Burkina Faso. *Earth* **2023**, *4*, 606–625. https://doi.org/10.3390/earth4030032

Academic Editor: Charles Jones

Received: 9 July 2023
Revised: 12 August 2023
Accepted: 16 August 2023
Published: 18 August 2023

1. Introduction

Climate change is a widely known global phenomenon whose impacts vary from region to region. The IPCC's *Sixth Assessment Report* clearly indicates that the increase in greenhouse gas (GHG) concentrations observed since 1850 is largely due to anthropogenic causes [1,2]. These effects are reflected in rising temperatures, more spatio-temporal variability in precipitation, and more severe and frequent extreme weather events (droughts, floods, etc.) [2].

It is also widely accepted that recent climate change, particularly in the Sahelian countries of West Africa, has altered annual and seasonal rainfall patterns and their spatial distribution [3]. Characterized by an arid to semi-arid climate in the Köppen–Geiger classification, the West African Sahel is considered by IPCC experts to be one of the world's most vulnerable regions to climate change and is expected to be the most affected in the world in the 21st century [4–12]. It has already experienced a temperature rise of 1 °C since 1950. Indeed, in 2021, temperatures in West Africa were 1.39 °C higher than in the period 1961–1990 [10–12].

Rainfall in the Sahel is characterized by high spatio-temporal variability, marked by strong seasonality: the rainy season begins in mid-spring (mid-April), followed by a gradual increase, reaching its peak around mid-August. Recurrent meteorological anomalies, such as droughts and floods, induce a wide range of effects on the environment and society [13–15] and have important implications for water resources [10–12], especially in Sahelian countries such as Burkina Faso, where water resources are already scarce.

This constant is even more acute in the Nakanbe–Wayen watershed, which is characterized by an arid environment and where climate variability already poses a major challenge for water supplies and agriculture, which is virtually dependent on rainfall and a source of income for over 80% of the country's working population [16].

Precipitation is therefore one of the most important meteorological variables for assessing the availability of water resources and must be analyzed on the basis of reliable information focusing on the spatial and temporal distribution of precipitation at the watershed scale [17–20].

Several studies have been conducted on climate variability and change [21–26] at the watershed scale. However, knowledge of the impacts of climate change on the availability of surface water resources in the Nakanbe–Wayen watershed remains limited.

As a matter of fact, this study aims to analyze the spatio-temporal dynamics of rainfall and determine its impact on the availability of water resources in the watershed, using climatic indices and geographic information systems. The results will provide scientific information for decision support to determine appropriate measures for strengthening adaptive capacity in the Nakanbe–Wayen watershed.

2. Materials and Methods

2.1. Study Area

The Nakanbe–Wayen watershed (Figure 1a) is located in the Sahelian zone between parallels 12°22′ and 14°06′ N and 0°47′ and 2°43′ W, and it occupies an area of 21,178 km^2 [27]. The relief of the watershed is relatively flat, with elevations ranging from 259 to 526 m, and an average of 324 m. The climate of the watershed is dry tropical, with a unimodal annual rainfall cycle (Figure 1b), characterized by a short wet season from June to September dominated by moist winds from the Gulf of Guinea, and a long dry season from November to May characterized by dust-laden harmattan winds from the northeast [27]. It covers two climatic zones: the Sahelian zone, with a total annual rainfall of between 300 and 600 mm, an average annual temperature of 29 °C, and average annual potential evapotranspiration (PTE) ranging from 3200 to 3500 mm; and the Sudano-Sahelian zone, with an average rainfall of between 600 and 900 mm, an average temperature of 28 °C, and average evapotranspiration of between 2600 mm and 2900 mm.

The basin's main river, the Nakanbe, rises in the northern part of the basin (Figure 1a), flows southwards, and only discharges during heavy rainfall in the rainy season. Annual maximum daily flows range from 43.1 to 230.0 m^3/s [27]. The Nakanbe–Wayen watershed, which is a sub-catchment of the Nakanbe river, contains a complex surface water system, including multiple river channels, lakes, and dams, and thus it plays a key role in economic and social development [28–30].

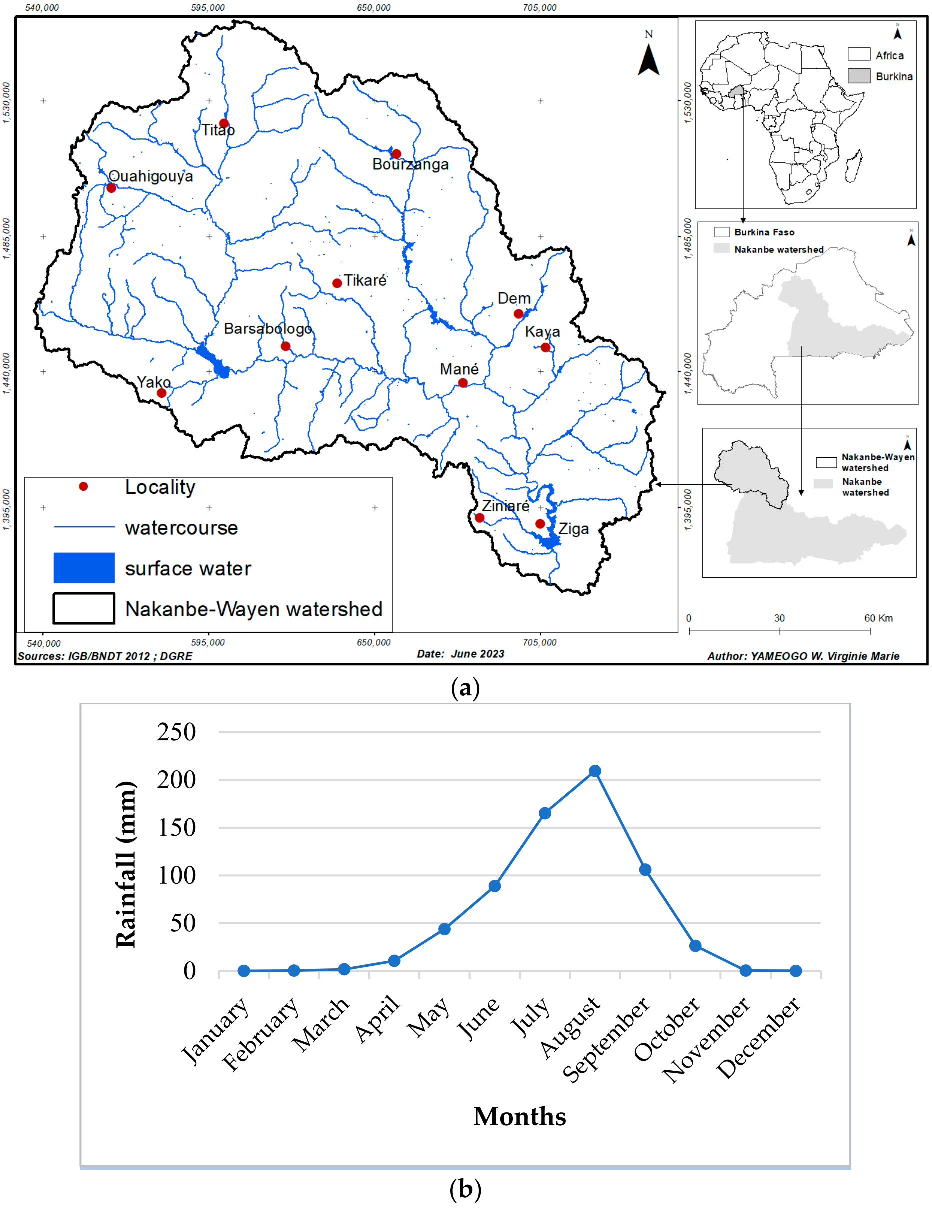

Figure 1. (**a**) Geographic location of the Nakanbe–Wayen watershed. (**b**) Annual rainfall cycle of the Nakanbe–Wayen watershed.

2.2. Data Sources

2.2.1. In Situ Data

Rainfall data were obtained from the National Meteorological Agency (ANAM) of Burkina Faso and cover the period 1981–2020. The rainfall data collected cover 14 stations, 13 of which are inside the basin and 1 of which is near the watershed. The geographical distribution of the stations is shown in Figure 2.

Unfortunately, many of the stations have numerous deficiencies (Table 1). However, the size criterion of the time series is important for the analysis of the changes [31]. In order to have a long time series of data, at daily time intervals, satellite precipitation datasets can be used as a complement or substitute for gauge station observations [32]. In this study, CHIRPS v2 spatialized products were used to fill gaps and missing data from in situ stations.

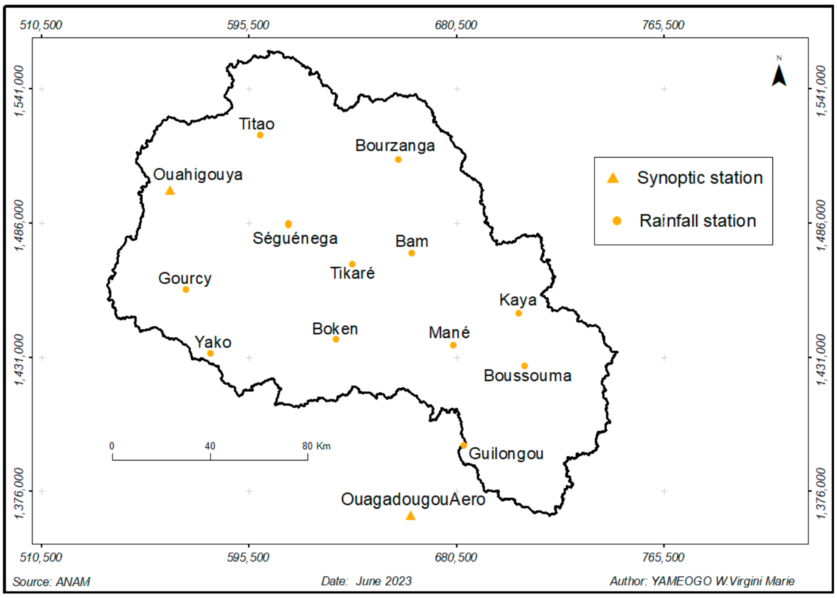

Figure 2. Location map of the meteorological stations studied in the Nakanbe–Wayen watershed.

Table 1. Selected climate stations in the Nakanbe–Wayen watershed.

	Station	Longitude (°)	Latitude (°)	Altitude (m)	Observation Available (%)
1	Bam	−1.50199	13.32601	264	61.3
2	Boken	−1.80365	13.00205	314	75
3	Bourzanga	−1.55029	13.67331	329	72.3
4	Boussouma	−1.07879	12.90471	323	69.4
5	Gourcy	−2.35498	13.19673	332	72.7
6	Guilongou	−1.30797	12.61320	315	69
7	Kaya	−1.09970	13.10015	313	60
8	Mane	−1.34636	12.98489	283	72.7
9	Ouahigouya *	−2.41651	13.56530	329	100
10	Seguenega	−1.96679	13.43784	307	72.7
11	Tikare	−1.72670	13.28709	400	59
12	Titao	−2.07208	13.76730	319	69.8
13	Yako	−2.26418	12.95827	294	66.4
14	Ouagadougou *	−1.51239	12.35641	303	100

* Synoptic station.

2.2.2. Gridded Climate Data

Due to a lack of ground-based observational data, satellite datasets can be used as an alternative to in situ observational data [26]. Precipitation data from the Climate Hazards Group Infrared Precipitation with Stations (CHIRPS) version 2, available since 1981, were selected from a set of commonly used satellite precipitation products. For this study, CHIRPS data were collected over the period 1981–2020. These satellite data, developed by the US Geological Survey (USGS) and the Climate Hazards Group at the University of California, Santa Barbara (UCSB), were chosen because of the availability of a longer series of data in near-real-time, reasonably high spatial (0.05° × 0.05°) and temporal (1 day) resolution, open access to the data, and their high frequency of use in Burkina Faso. Furthermore, these datasets, widely used in previous studies in Burkina Faso and in West Africa, have shown good correlations with in situ observational datasets [33–38]. They integrate satellite data with in situ station data to create gridded time series datasets of near-global precipitation at daily time steps and a 5.3 km (0.05°) resolution [34,36,38].

2.3. Methods

2.3.1. Data Extraction and Dataset Validation

The extraction of meteorological data covering the study area was made according to the geographical coordinates of the 14 in situ stations in the watershed (Figure 2). Each measuring point contains a time series of precipitation data from 1 January 1981 to 31 December 2020. The performance of the CHIRPS datasets was assessed by comparing these data to those of in situ stations with missing data of less than 10% over the period considered, and a long series of at least 30 years. Only the synoptic stations of Ouahigouya and Ouagadougou met the criteria mentioned above. The performance evaluation method used included the statistical indicators summarized in Table 2.

Table 2. Statistical indicators for validation of climatic data.

Statistical Indicator	Formula	Values Range	Perfect Score	Equation
Pearson correlation coefficient	$r = \frac{\sum_{i=1}^{n}(G_i - G)(S_i - S)}{\sqrt{\sum_{i=1}^{n}\left(G_i - \overline{G}\right)^2}\sqrt{\sum_{i=1}^{n}\left(S_i - \overline{S}\right)^2}}$	−1 to 1	1	(1)
Mean error (ME)	$ME = \frac{1}{n}\sum_{i=1}^{n}(S_i - G_i)$	−∞ to ∞	0	(2)
Bias	$Bias = \frac{\sum_{i=1}^{n} S_i}{\sum_{i=1}^{n} G_i}$	0 to ∞	1	(3)
Root mean square error (RMSE)	$RMSE = \sqrt{\frac{1}{n}\sum_{i=1}^{n}\left(S_i - G_i\right)^2}$	0 to ∞	0	(4)
Nash–Sutcliffe efficiency coefficient	$E = 1 - \frac{\sum_{i=1}^{n}\left(S_i - G_i\right)^2}{\sum_{i=1}^{n}\left(G_i - G\right)^2}$	−∞ to 1	1	(5)
Probability of detection	$POA = H/(H + M)$	0 to 1	1	(6)
False alarm ratio	$FAR = F/(H + F)$	0 to 1	0	(7)

G_i gauge rainfall measurement; $\overline{G}$: average gauge rainfall measurement; S_i: satellite rainfall estimate; $\overline{S}$: average satellite rainfall estimate; n: number of data pairs; H: number of hits; F: number of false alarms; and M: number of misses.

In this study, the performance of CHIRPS satellite rainfall product estimates was examined at monthly scales for the period 1981 to 2020. Due to the poor performance reported in previous studies, no daily comparisons were made [34,39].

2.3.2. Quality Control and Homogenization

Due to consistency issues that may have existed in the collection, recording, and storage of data, thorough quality control and assessment of the homogeneity of the data prior to data analysis were required in order to eliminate erroneous daily precipitation data as well as to identify artificial jumps in the time series. For this purpose, the quality control and data homogenization tools RHTest of RClimDex (version 5.0) were used.

- Quality control

Quality control (QC) examines the data for negative precipitation values [33]. No such situations were observed. QC also detects precipitation outliers. Outliers are daily values outside a user-defined threshold [40]. Outliers identified as artifacts were replaced by missing values in the observed data time series.

- Homogenization

The homogeneity of the dataset was assessed in RclimDex using RHTest to detect points of change in the dataset. No significant changes were found.

After ensuring these checks, the station data were assumed to be 100% consistent for further processing [41].

2.3.3. Analysis of Climate Extremes Indices Using RClimDex

The ETCCDI (Expert Team on Climate Change Detection and Indices) of the World Meteorological Organization (WMO) has recommended 27 climate indices to assess changes in precipitation and temperature patterns in terms of duration, intensity, and occurrence [31,42,43]. For this study, RclimDex software facilitated the calculation of 10 indices (Table 3) considered relevant to assess the impact of climate change on the availability of water resources, such as intensity, frequency, and duration of precipitation indices.

Table 3. List of precipitation indices used.

Indices	Descriptive Name	Definition	Units
PRCPTOT	Annual total wet-day precipitation	Annual total rainfall from days $\geq$ 1 mm	mm
Rx1day	Max 1-day precipitation amount	Annual maximum 1-day precipitation	mm
Rx5day	Max-5-day precipitation amount	Annual maximum consecutive 5-day rainfall	mm
CDD	Consecutive dry days	Maximum number of consecutive days with rainfall < 1 mm	days
CWD	Consecutive wet days	Maximum number of consecutive days with rainfall $\geq$ 1 mm	days
R20mm	Number of heavy precipitation days	Annual counts of days when rainfall $\geq$ 20 mm	days
R50mm	Number of very heavy precipitation days	Annual counts of days when rainfall $\geq$ 50 mm	days
R95p	Very wet days	Annual total precipitation from the days with daily rainfall > 95th percentile	mm
R99p	Extremely wet days	Annual total precipitation on the days when daily rainfall > 99th percentile	mm
SDII	Simple daily intensity index	Annual total rainfall when (PRCP $\geq$ 1 mm) divided by the number of wet days	mm/day

2.3.4. Trend Analysis

Linear trends in precipitation (P) were analyzed using Mann–Kendall tests [44] coupled with the Sen slope estimator [45]. The Mann–Kendall test is a non-parametric test recommended by the World Meteorological Organization to test for the presence of trends in time series [46]. It is considered a robust linear trend regression method [45,47–50]. The Mann–Kendal test (Z Kendall coefficient) provides information on the significance of the trend [46]. This method is widely used in climate and hydrological studies [4,51–56]. Thus, there is a trend if the *p*-value is less than 5%. Sen's slope estimator [6] was used to estimate both the magnitude of the linear trend and its direction. It is a non-parametric method of calculating the slope of the median. It allows for a more reliable assessment of the trend [56].

2.3.5. Spatial Interpolation

The kriging linear interpolation method was used to analyze the spatial distribution of average precipitation at the watershed scale. This interpolation method is recognized as the most distinct interpolation method for interpolating meteorological datasets [57,58]. This geospatial interpolation method is based on statistical models including autocorrelation, i.e., the statistical relationships between measured points. This method is also an advanced and sophisticated geostatistical procedure that generates and estimates a statistical surface from a set of scattered points [59]. In general, kriging forms weights around measured values to predict values at unmeasured locations [60].

3. Results

3.1. Data Validation

In this study, the performance of CHIRPS satellite rainfall product estimates was examined at monthly scales for the period 1981 to 2020 on the basis of various statistical performance evaluation criteria, as listed in Table 2.

The performance evaluation statistics of these products gave good agreement with the in situ data (Table 4). Better correlation coefficients (r > 90%), bias (between 1.004 and 1.05), NSE (≥83%), and RMSE (between 27 and 32 mm/month) were found. This implies that CHIRPS satellite rainfall data performed well over the Nakanbe–Wayen watershed.

Table 4. Results of statistical tests.

Name	Ouagadougou	Ouahigouya
Pearson correlation coefficient (r)	0.95	0.92
BIAS	1.05	1.03
ME *	3.37	1.53
RMSE *	27.1	32.66
Nash–Sutcliffe efficiency NSE	0.89	0.83
POD	0.97	0.96
FAR	0.13	0.12

* ME and RMSE are in mm/month. The other indicators are unitless.

3.2. Average Annual Precipitation

The rainfall regime of the Nakanbe–Wayen watershed was marked by strong spatio-temporal variability. Cumulative rainfall in the basin varied between 268.20 mm and 1170.10 mm, with an average of 640.03 mm, from 1981 to 2020. The rates of variation ranged from 25% to 16%, with an average of 20% (Table 5).

Table 5. Descriptive statistics of cumulative rainfall from 1981 to 2020 in the Nakanbe–Wayen basin.

Station	Minimum (mm)	Maximum (mm)	Average (mm)	Standard Deviation (mm)	Coefficient of Variation (%)
Bam	425.3	1033.14	636.58	130.06	20.43
Bourzanga	355.7	742.8	564.75	92.54	16.38
Seguenega	362.41	1000	621.41	140.72	22.64
Titao	268.2	762	517.99	127.55	24.62
Boussouma	370.9	1170.1	675.63	154.59	22.88
Gourcy	446.91	1016	688.2	149.44	21.71
Guilongou	517.98	972.7	707.15	117.72	16.66
Kaya	466.2	959.8	655.57	133.84	20.41
Mane	458.6	1110.1	674.87	136.98	20.29
Ouahigouya	358.2	983.4	679.95	172.1	25.31
Tikare	400.9	1000	638.79	129.91	20.33
Yako	459.34	1090.6	695.02	136.61	19.65
Boken	398.1	931.5	619.42	124.01	20.02
Average			640.03		20.02

At the same time, a significant upward trend in mean annual precipitation was detected at almost all stations for the period 1981–2020 (Figure 3a). Only one station showed a non-significant (p-value = 0.35) upward trend. The rate of increase ranged from 1.68 mm/year to 9.08 mm/year. The trend in average annual rainfall in the Nakanbe–Wayen watershed is shown in Figure 3b.

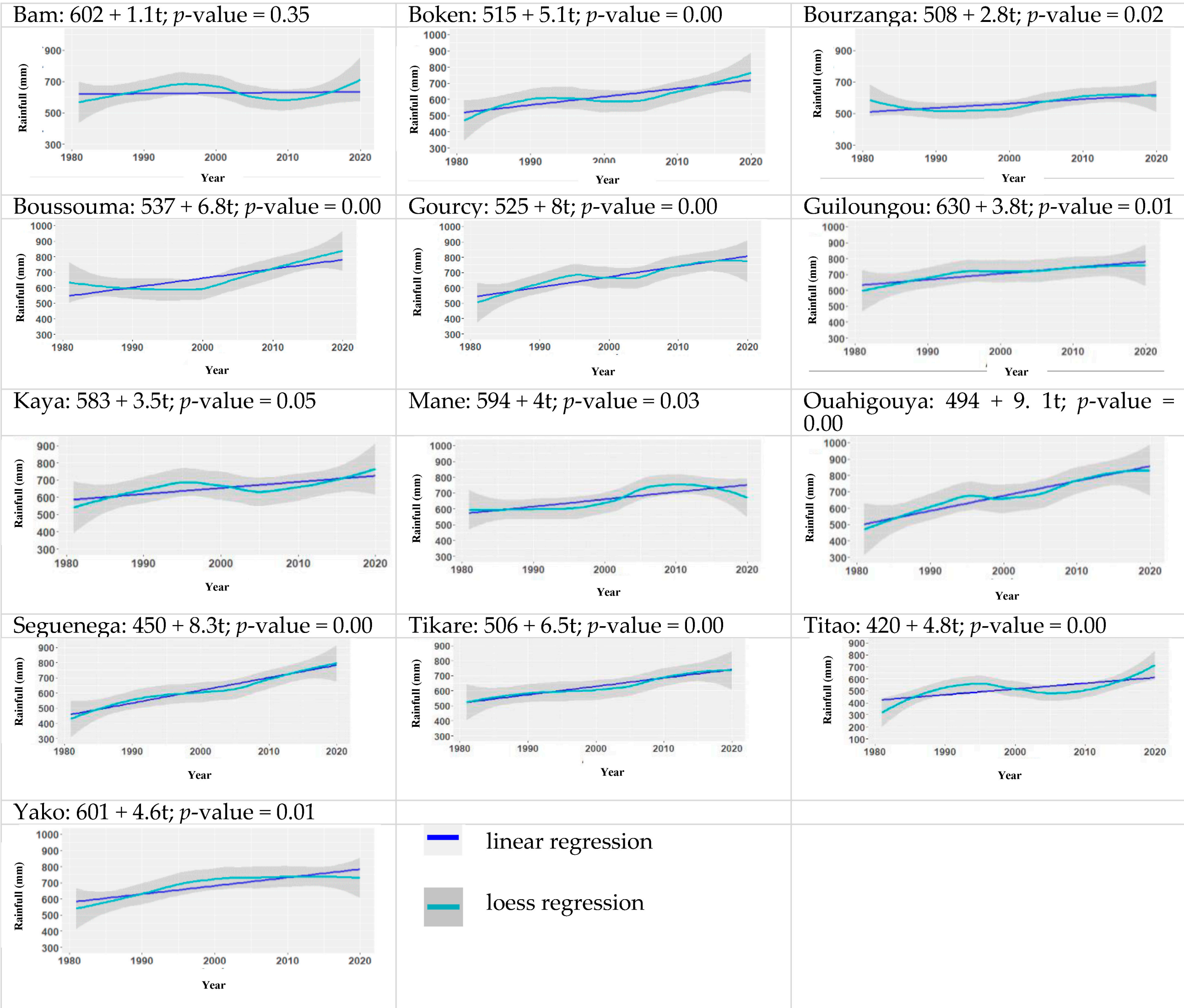

(**a**)

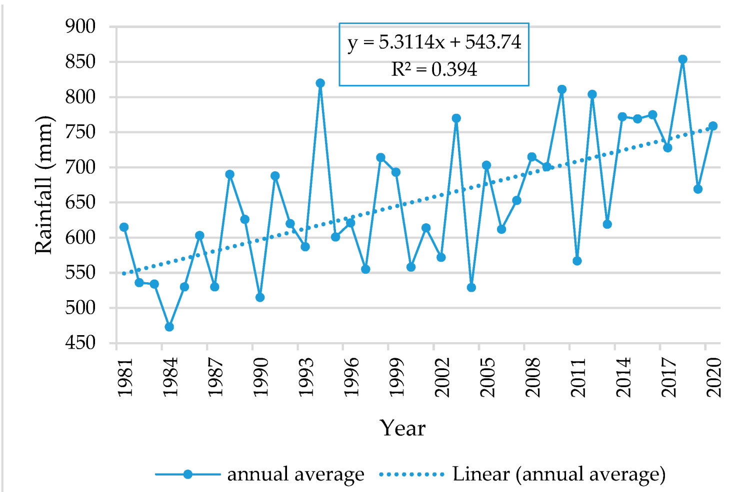

(**b**)

Figure 3. (**a**) Rainfall trend station-by-station in the Nakanbe–Wayen watershed (t = time). (**b**) Average annual rainfall trend in the Nakanbe–Wayen watershed.

3.3. Analysis Spatio-Temporal Evolution of Extreme Precipitation Trends

3.3.1. Temporal Trends

- Total Annual Precipitation per Rainy Day (PRCPTOT) and Simple Rainfall Intensity (SDII)

Trend analysis of total annual precipitation per rainy day (PRCPTOT) showed a significant (5% significance level) upward trend at all meteorological stations in the watershed over the 1981–2020 period (Figure 4 and Table 6). Only one station (Bam) showed a non-significant (*p*-value = 0.35) increasing trend. The rate of increase ranged from 1.68 mm/year (or 16.8 mm/decade) to 9.08 mm/year (or 90.8 mm/decade), with an average rate of 5.29 mm/year (or 52.9 mm per decade). Additionally, the PRCPTOT index showed a similar trend to the average annual precipitation.

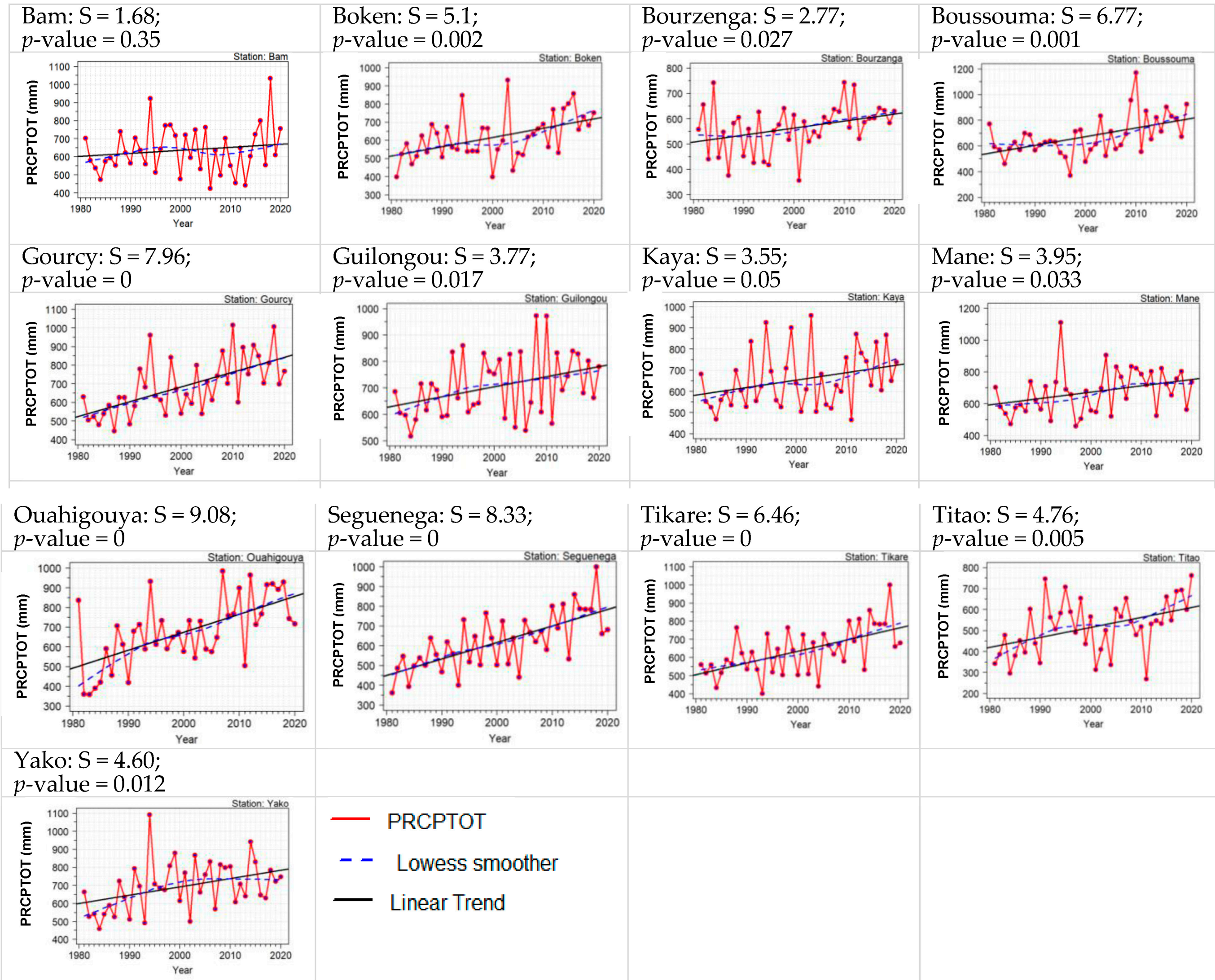

Figure 4. Trends in total annual rainfall per day (PRCPTOT) in the Nakanbe–Wayen watershed. S = Slope (mm/year).

Moreover, trend analysis of simple rainfall intensity (SDII) showed a significant upward trend at all climate stations in the watershed over the 1981–2020 period (Figure 5 and Table 6). The rate of increase in simple rainfall intensity ranged from 0.09 to 0.36 mm/day per year, with an average increase of 0.23 mm/day per year. Only the Bourzanga station showed a significant (*p*-value = 0.00) downward trend, with a rate of decrease of −0.12 mm/day per year.

Table 6. Statistical significance of the linear regression model assessed using the Mann–Kendall test and Sen's slope values of extreme precipitation indices from 1981 to 2020 for stations in the Nakanbe–Wayen watershed.

Index Station	PRCP TOT (mm/Year)	SDII (mm/Day/Year)	CDD (Days/Year)	CWD (Days/Year)	R20 mm (Days/Year)	R50 mm (Days/Year)	Rx1day (mm/Year)	Rx5day (mm/Year)	R95p (mm/Year)	R99p (mm/Year)
Bam	1.68	0.10 *	0.27	−0.02	0.1	0.02	0.22	0.25	1.79	1.25
Bourzanga	2.77 *	−0.12 **	−0.61 *	0.07 **	−0.14 **	−0.03	−0.43	−0.53	−3.04 *	−1.02
Boussouma	6.77 **	0.25 **	0.24	−0.04 *	0.26 **	0.05 *	0.98 *	1.45 **	5.86 **	2.30 *
Gourcy	7.96 **	0.27 **	0.34	−0.04	0.29 **	0.07 **	1.3 **	1.45 **	6.71 **	3.23 **
Guilongou	3.77 *	0.19 **	0.43	−0.06 **	0.22 **	0.06 **	0.37	0.46	4.48 **	1.31
Kaya	3.55 *	0.15 **	0.3	−0.04 *	0.17 **	0.02	0.46	0.46	3.75 *	0.42
Mane	3.95 **	0.24 **	0.68 *	−0.03 *	0.22 **	0.04 *	0.58	1.04 *	3.43 *	0.35
Ouahigouya	9.08 **	0.13 **	−0.19	−0.01	0.20 **	0.05 **	0.63 *	0.73	3.97 **	0.75
Seguenega	8.33 **	0.37 **	0.26	−0.03	0.31 **	0.05 **	1.08 **	1.73 **	5.77 **	2.15 *
Tikare	6.46 **	0.34 **	0.82 *	−0.04 *	0.29 **	0.04 **	0.82 **	1.44 **	5.46 **	1.93 *
Titao	4.76 **	0.27 **	0.85 **	−0.04	0.21 **	0.04 **	1.10 **	1.19 **	4.65 **	0.99
Yako	4.60 *	0.12 **	0.19	−0.01 *	0.19 **	0.02	0.85 *	1.22 *	2.41	1.03
Boken	5.1 **	0.32 **	0.60 *	−0.06 **	0.04	0.05 **	1.08 **	1.07 *	5.36 **	2.19 **

The character * indicates a significance ≤ 5%; ** indicates a significance ≤ 1%, and the absence of a character indicates a significance ≥ 5%.

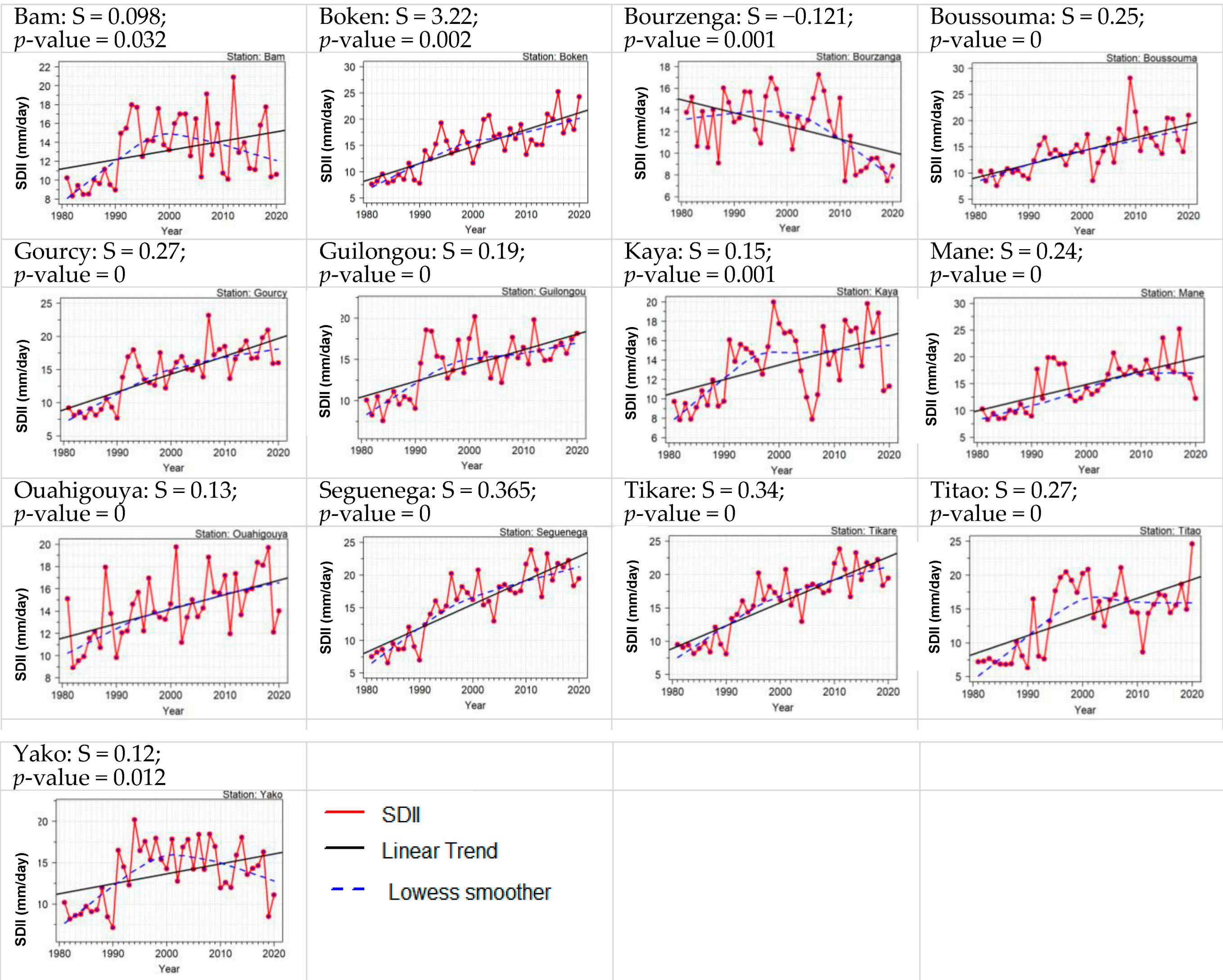

Figure 5. Trend of the simple precipitation intensity index (SDII). S = Slope (mm/day/year).

- Consecutive dry days (CDD) and consecutive wet days (CWD)

The analysis of consecutive dry days (CDD) indicated an increasing trend in 85% of the stations, of which 40% were statistically significant, with a magnitude of 0.19 days/year (i.e., 1.9 days/decade) to 0.85 days/year (i.e., 8.5 days/decade). The average rate of increase was 0.45 days/year (or 4.5 days/decade). Only 15% of the stations showed a decreasing trend of −0.19 days/year (or −1.9 days/decade) and −0.6 days/year (or −6 days/decade), respectively (Figure 6 and Table 6).

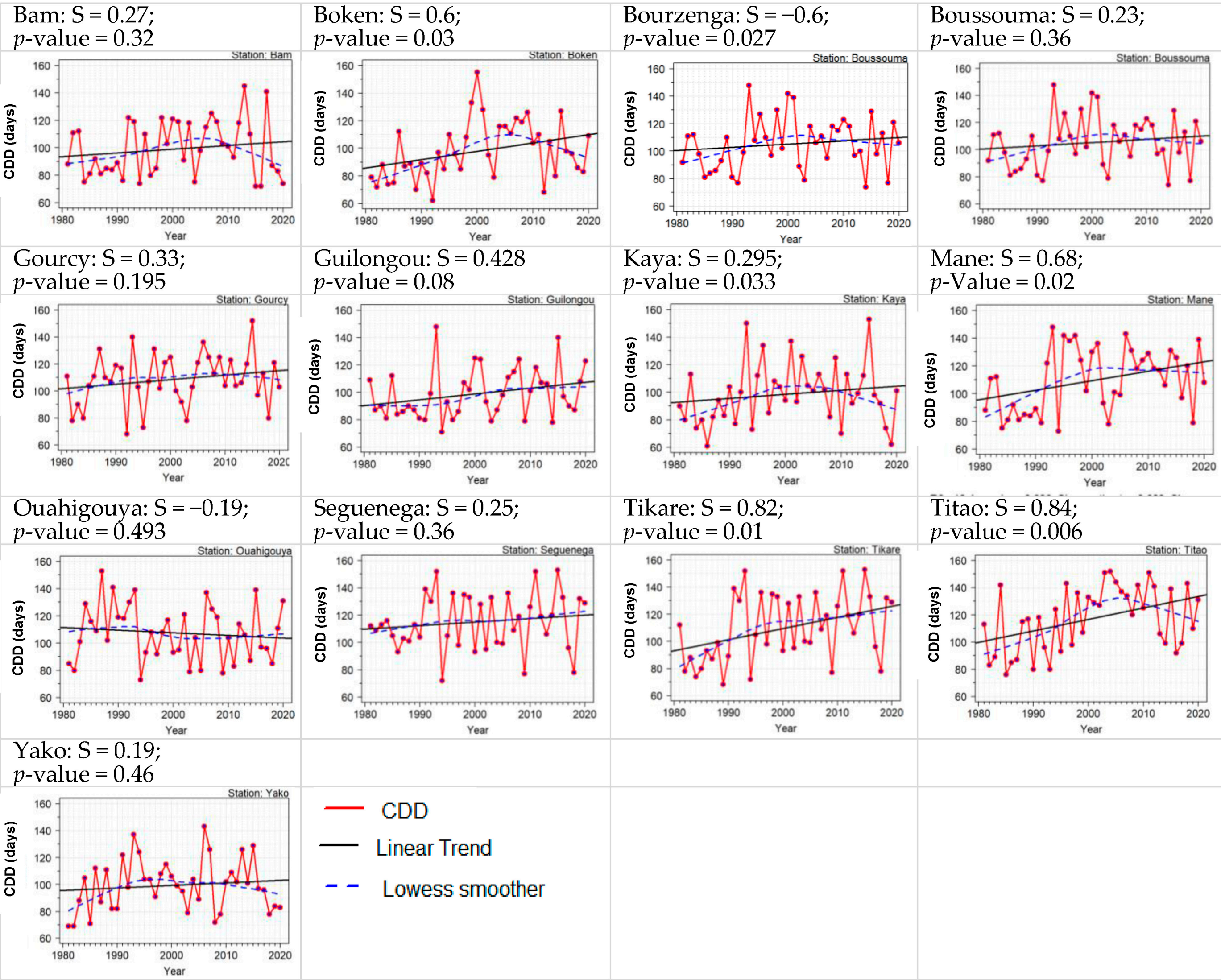

Figure 6. Trend of consecutive dry days (CDD). S = Slope (days/year).

At the same time, the number of consecutive wet days CWD was found to be decreasing at 92% of the meteorological stations in the watershed, of which 42% of the stations were statistically significant, with a magnitude ranging from 0.02 days/year (i.e., 0.2 days/decade) to 0.06 days/year (i.e., 0.6 days/decade), and an average of 0.030 days/year (i.e., 0.3 days/decade) for all stations. Only one station (Bourzanga) showed a significant upward trend of 0.07 days/year, or 0.7 days/decade (Figure 7 and Table 6).

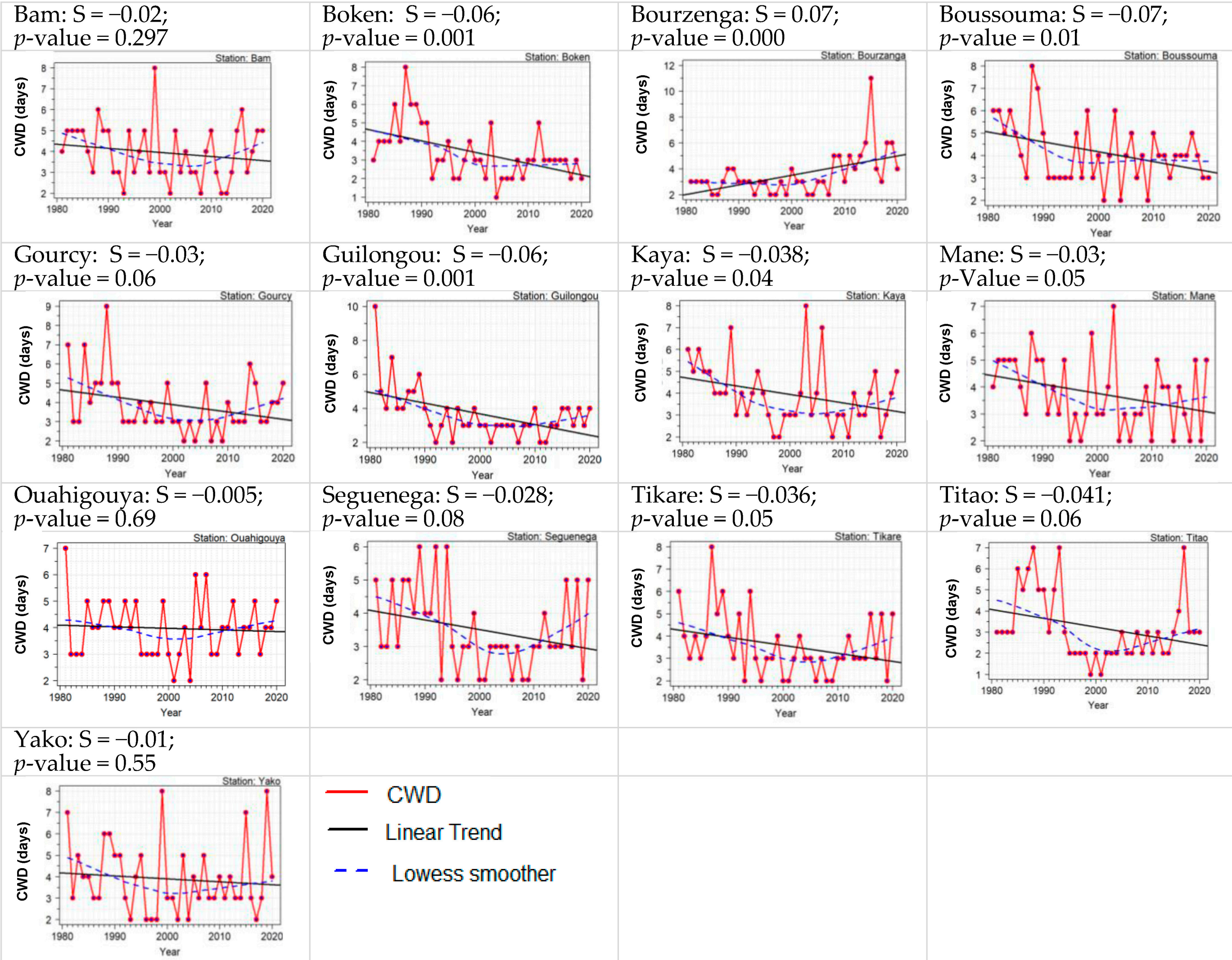

Figure 7. Trends in consecutive wet days (CWD). S = Slope (days/year).

- Number of heavy (R20mm) to very heavy (R50mm) rainfall days.

The annual number of heavy precipitation days with precipitation $\geq$ 20 mm (R20 mm) increased at 92% of the weather stations in the watershed, with 85% of the stations being statistically significant (Figure 8 and Table 6). The average rate of increase was 0.20 days/year (or 2 days/decade). Only one station (Bourzanga) showed a significant downward trend of $-$0.135 days/year (or $-$1.35 days/decade).

At the same time, almost all stations, or 92%, showed a significant upward trend in the number of days with very heavy rainfall of $\geq$50 mm (Table 6), with 75% of stations being statistically significant. The average rate of increase was 0.04 days/year (or 0.4 days/decade). Only one station (Bourzanga) showed a non-significant decreasing trend.

- Maximum 1-day (Rx1day) and 5-day (Rx5day) precipitation

The maximum 1-day precipitation (Rx1day) and the maximum consecutive 5-day precipitation (Rx5day) showed an increasing trend in 92% of the meteorological stations in the watershed, of which 62% were statistically significant (Figure 9 and Table 6). The rate of increase was between 0.22 mm/year and 1.3 mm/year, with an average increase of 0.79 mm/year (i.e., 7.9 mm/decade) for the Rx1day index, while that of the Rx5day index was between 0.25 mm/year and 1.45 mm/year, with an average of 1.04 mm/year (i.e., 10.4 mm/decade). Only one station (Bourzanga) showed a non-significant (p-value $\geq$ 0.05) decreasing trend, with a magnitude of −4 mm/decade and −5 mm/decade for Rx1day and Rx5day, respectively.

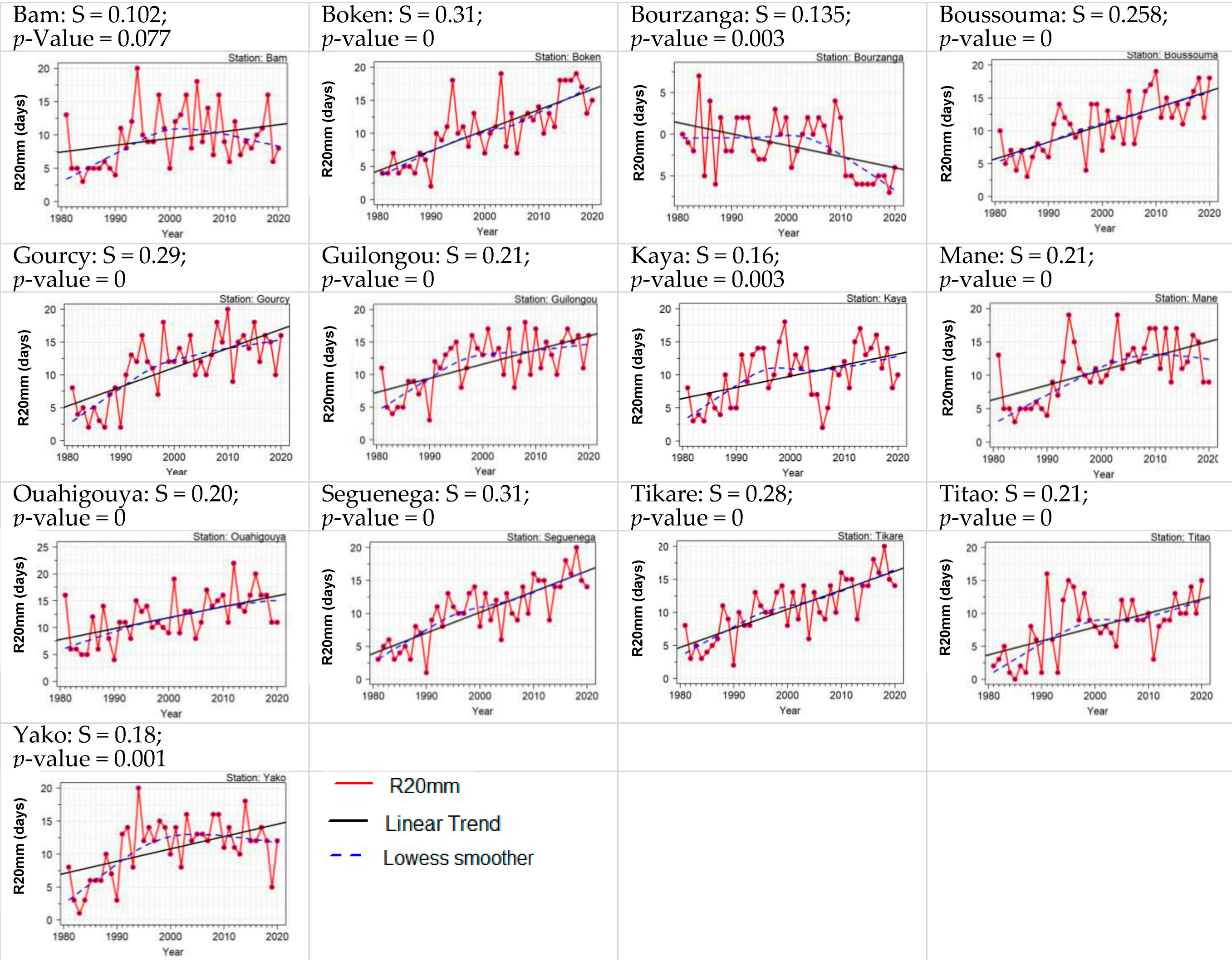

Figure 8. Trends of number of heavy precipitation days (R20 mm). S = Slope (days/year).

- Very wet days (R95p) and extremely wet days (R99p)

Very wet (R95p) to extremely wet (R99p) days showed increasing trends at 92% of weather stations in the watershed, with 83% and 42% of stations statistically significant for R95p and R99p, respectively (Table 6). The rate of increase in R95p ranged from 1.79 to 6.71 mm/year (i.e., 17.9 to 67.1 mm/decade), with an average increase of 4.47 mm/year (i.e., 44.7 mm/decade) (Figure 10), while that of R99p ranged from 1.25 mm/year to 2.30 mm/year, with an average of 1.45 mm/year (i.e., 14.5 mm/decade). Only one station (Bourzanga) showed a non-significant downward trend (Table 6).

3.3.2. Spatial Distribution Trends

The spatial distribution of total precipitation per day (PRCPTOT) was heterogeneous and increased along the north–south gradient (Figure 11a), with lower precipitation in the north and higher in the southern part of the watershed. Additionally, the north of the basin had the lowest values of simple precipitation intensity (SDII), and the northeast and southeast had high values (Figure 11b). Unlike the spatial distribution of total precipitation per day (PRCPTOT), that of consecutive dry days (CDD) followed a south–north cross gradient (Figure 11c). Where rainfall was low, the number of consecutive dry days was high and vice versa. As for the spatial distribution of consecutive wet days (CWD) (Figure 11d), it grew inversely parallel to that of the simple precipitation intensity (SDII). This means that where the simple precipitation intensity was high, the number of consecutive wet days was low. Additionally, the spatial distribution of the number of days with heavy rainfall (R20mm) and very heavy rainfall (R50mm) (Figure 11e,f), as well as that of very wet (R95p) to extremely wet (R99p) days (Figure 11g,h), were also nearly similar, growing along a north–south gradient, as was the distribution of total rainfall per wet day. As for the spatial distributions of maximum 1-day (Rx1day) and 5-day (Rx5day) precipitation (Figure 11i,j), they were similar, with the highest values located in the southeast and the average values in the northeast.

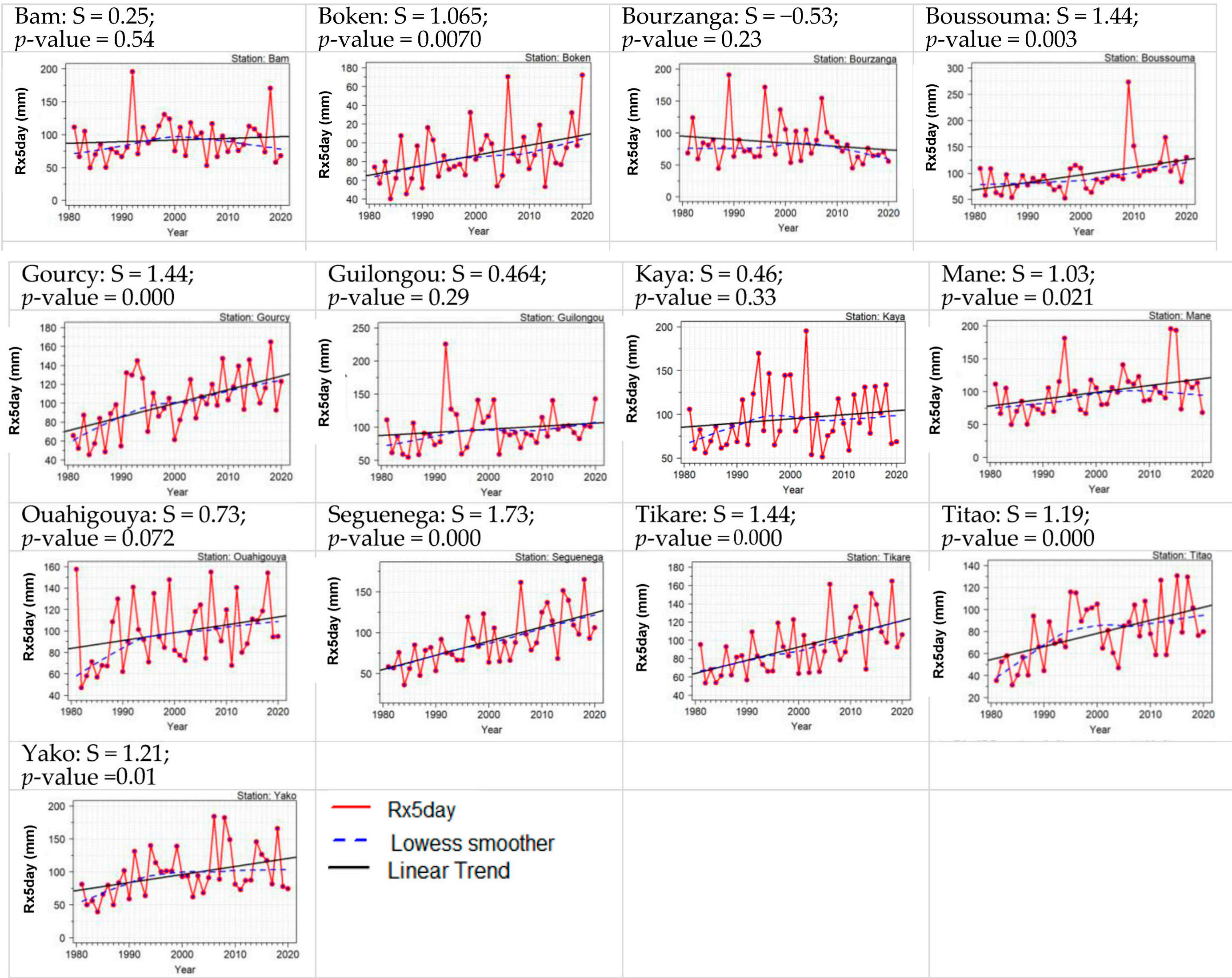

Figure 9. Trends in maximum 5-day (Rx5day) precipitation. S = Slope (mm/year).

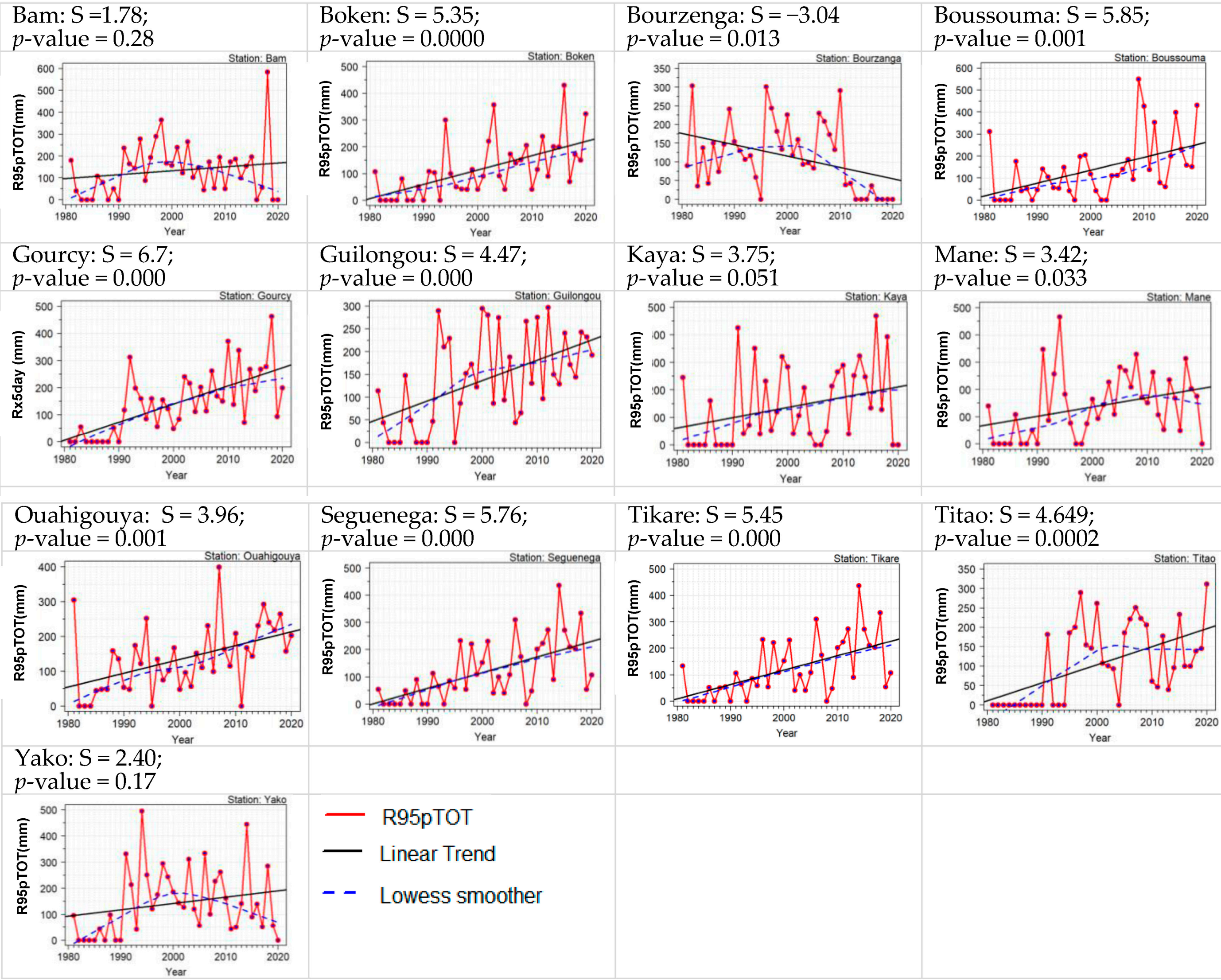

Figure 10. Trends in very wet days (R95p). S = Slope (mm/year).

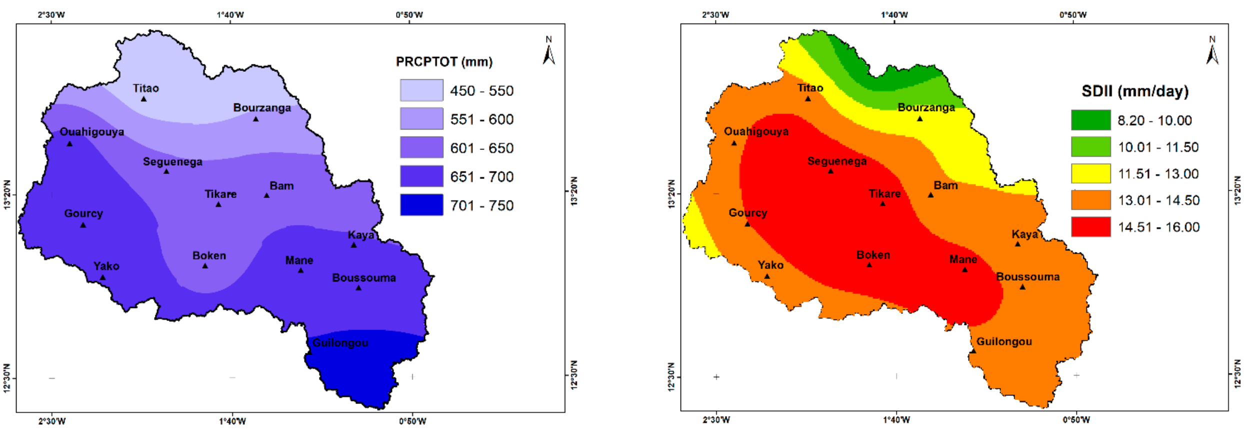

(**a**) Total annual precipitation per rainy day (PRCPTOT) (**b**) Simple precipitation intensity (SDII)

Figure 11. *Cont.*

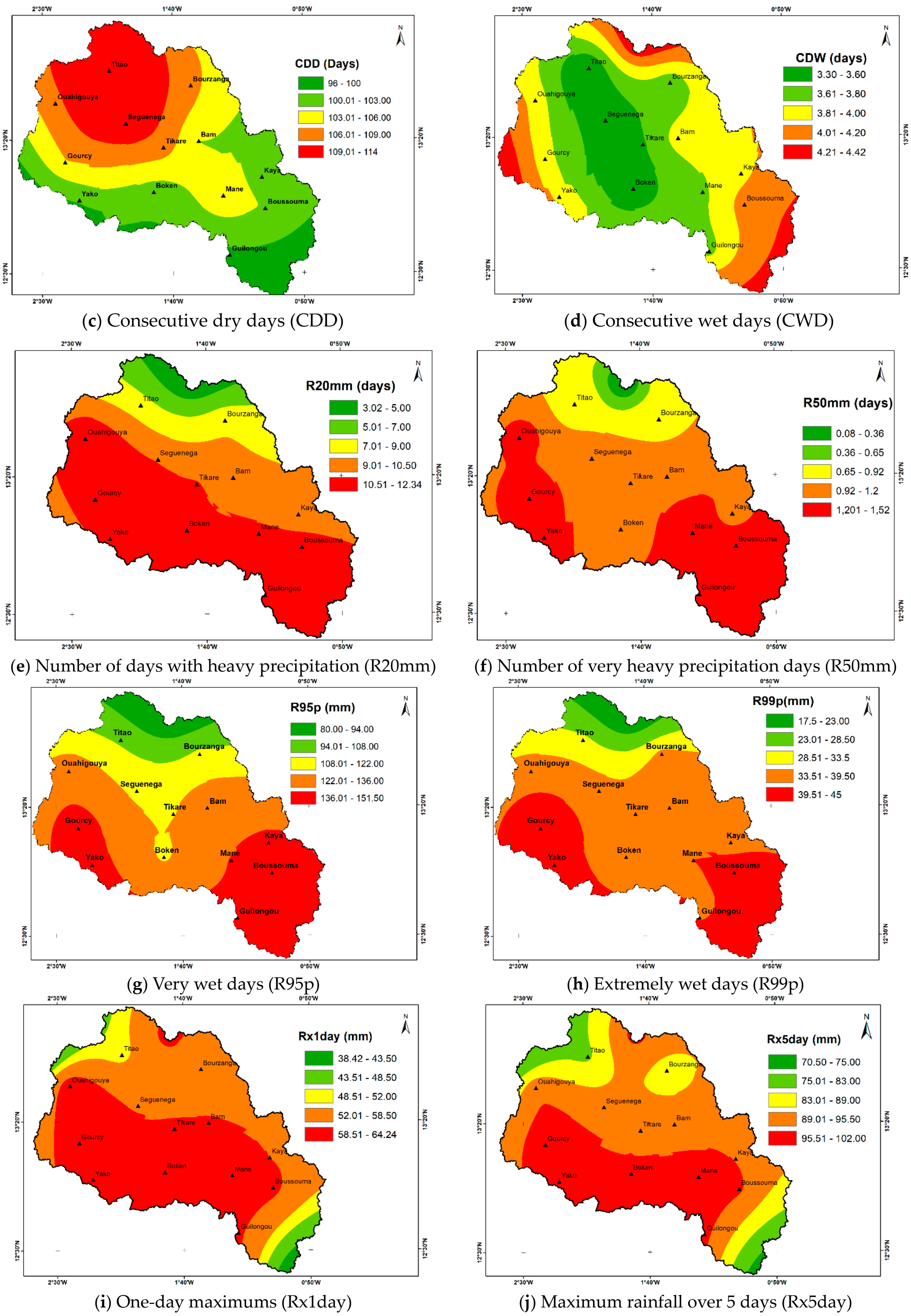

Figure 11. Spatial distribution of extreme precipitation indices in the Nakanbe–Wayen watershed.

4. Discussion

Precipitation indices have been widely used to analyze changes in the spatio-temporal distribution of precipitation and their impact on the availability of water resources, as well as for socio-economic and environmental issues [9]. This study, conducted in the Nakanbe–Wayen watershed, provided insight into the effects of climate change on the availability of surface water resources in the watershed.

The cumulative annual precipitation and the PRCPTOT index show a significant upward trend in almost all the meteorological stations of the watershed over the 1981–2020 period. These results are in agreement with the study by Gbohou [23], which notes an increase in rainfall in the same watershed. These results are also in line with national trends [61]. Several authors believe that this recent increase in precipitation is probably due to the warming of the northern Atlantic Ocean, which may have attracted summer rains further north, thus increasing precipitation in the Sahel [62–64].

At the same time, the simple rainfall intensity index (SDII), the annual number of days with heavy to very heavy rainfall (R20 mm, R50 mm), the maximum one-day rainfall (Rx1day), the maximum consecutive 5-day rainfall (Rx5day), and the occurrence of very rainy days (R95) and extremely rainy days (R99) increased at almost all weather stations in the watershed. The increase in the frequency and intensity of extreme precipitation events noted in the watershed corroborates the results of previous studies, which show that these extreme events have become more frequent and more intense in the West African Sahel [65,66].

These new precipitation conditions will most likely be maintained by global warming [65,67]. This upward trend in extreme precipitation also increases the risk of flooding [68], damaging water storage infrastructure and essential services, and impacting water availability.

Concomitant with the increase in extreme rainfall, the upward trend in drought occurrence, illustrated by the CDD index (number of consecutive dry days), increased at all stations, while the CWD index (number of consecutive rainy days) also decreased at all stations in the catchment. This reflects a shortening of wet periods and a lengthening of dry periods. This trend towards more frequent dry spells has also been demonstrated by [65], inducing a rainfall deficit, reducing water availability [69], and leading to increased water stress.

Because water is the primary means by which climate change affects populations, the environment, and economies, water and climate change crises are regularly cited as among the most serious crises facing humanity in the coming decades. They are among the major issues of the 21st century, and the social repercussions and impacts of water scarcity are likely to be severe. This calls for a new, intelligent approach to water resource management in the face of climate change. To achieve this, it will be essential to set up a water observatory for the Nakanbe–Wayen watershed to ensure the rational management of this fragile and limited resource in order to meet the demand for water in a context of changing climatic conditions.

5. Conclusions

The present study analyzed changes in rainfall distribution and identified extreme rainfall events based on climatic indices in the Nakanbe–Wayen watershed. The spatial analysis of rainfall indices showed heterogeneity in the distribution of the rainfall. The rainfall indices showed an upward trend in precipitation. On the other hand, a positive trend prevalence, i.e., an increase in the intensity and occurrence of extreme rainfall events (SDII, Rx1day, Rx5day, R95p, R99p, R20 mm, R50 mm) in the basin was also recorded. At the same time, a trend towards increasing periods of drought was observed.

In light of these analyses, it should also be noted that the increase in rainfall observed in the Nakanbe–Wayen watershed was consecutive to the increase in the intensity and frequency of extreme rainfall events. This is because the trend towards higher rainfall in the watershed occurred despite shorter wet periods and longer dry periods. Water stress and water-related hazards, such as devastating droughts and floods, have major impacts on communities and ecosystems.

In these conditions of vulnerability, the development of an appropriate and anticipatory management strategy for climate risks related to water resources at the watershed scale is essential. This should be formulated in a participatory scheme involving all stakeholders; integrating science, governance, and society; and focusing on rainfall distribution and water resource availability.

Author Contributions: Conceptualization, W.V.M.Y., Y.L.A. and J.H.D.; methodology, W.V.M.Y., Y.L.A. and J.H.D.; writing, W.V.M.Y.; revision, M.H., J.H.D., Y.L.A., F.T., B.T., Z.S., O.K.; supervision, M.H., J.H.D. and Y.L.A. All authors have read and agreed to the published version of the manuscript.

Funding: This research received no external funding.

Data Availability Statement: The raw data supporting the conclusions of this article will be made available by the authors without undue reservation.

Conflicts of Interest: The authors declare no conflict of interest.

References

1. IPCC. *Climate Change 2014: Impacts, Adaptation, and Vulnerability; Part A: Global and Sectoral Aspects*; Contribution of Working Group II to the Fifth Assessment Report of the Intergovernmental Panel on Climate Change; Field, C.B., Barros, V.R., Dokken, D.J., Mach, K.J., Mastrandrea, M.D., Bilir, T.E., Chatterjee, M., Ebi, K.L., Estrada, Y.O., Genova, R.C., et al., Eds.; Cambridge University Press: Cambridge, UK; New York, NY, USA, 2014; 1132p. Available online: https://www.ipcc.ch/site/assets/uploads/2018/02/WGIIAR5-PartA_FINAL.pdf (accessed on 10 January 2023).
2. IPCC. Summary for Policymakers. In *Climate Change 2023: Synthesis Report: A Report of the Intergovernmental Panel on Climate Change*; Contribution of Working Groups I, II and III to the Sixth Assessment Report of the Intergovernmental Panel on Climate Change; Lee, H., Romero, J., Eds.; IPCC: Geneva, Switzerland, 2023; 36p.
3. Banerjee, A.; Chen, R.; EMeadows, M.; Singh, R.B.; Mal, S.; Sengupta, D. An Analysis of Long-Term Rainfall Trends and Variability in the Uttarakhand Himalaya Using Google Earth Engine. *Remote Sens.* **2020**, *12*, 709. [CrossRef]
4. Mougin, É.; Hiernaux, P.; Kergoat, L.; Grippa, M.; De Rosnay, P.; Timouk, F.; Le Dantec, V.; Demarez, V.; Lavenu, F.; Arjounin, M. The AMMA-CATCH Gourma observatory site in Mali: Relating climatic variations to changes in vegetation, surface hydrology, fluxes and natural resources. *J. Hydrol.* **2009**, *375*, 14–33. [CrossRef]
5. Lebel, T.; Cappelaere, B.; Galle, S.; Hanan, N.; Kergoat, L.; Levis, S.; Vieux, B.; Descroix, L.; Gosset, M.; Mougin, E. AMMA-CATCH studies in the Sahelian region of West-Africa: An overview. *J. Hydrol.* **2009**, *375*, 3–13. [CrossRef]
6. Boubacar, I.; Karambiri, H.; Polcher, J.; Hamma, Y.; Ribstein, P. Changes in rainfall regime over Burkina Faso under the climate change conditions simulated by 5 regional climate models. *Clim. Dyn.* **2014**, *42*, 1363–1381.
7. Frappart, F.; Hiernaux, P.; Guichard, F.; Mougin, E.; Kergoat, L.; Arjounin, M.; Lavenu, F.; Koité, M.; Paturel, J.-E.; Lebel, T. Rainfall regime across the Sahel band in the Gourma region, Mali. *J. Hydrol.* **2009**, *375*, 128–142. [CrossRef]
8. Oguntunde, P.G.; Abiodun, B.J.; Lischeid, G. Impacts of climate change on hydro-meteorological drought over the Volta Basin, West Africa. *Glob. Planet. Chang.* **2017**, *155*, 121–132. [CrossRef]
9. IPCC. *Africa, Climate Change 2014—Impacts, Adaptation and Vulnerability: Part B: Regional Aspects: Working Group II Contribution to the IPCC Fifth Assessment Report: Volume 2: Regional Aspects*; Intergovernmental Panel on Climate Change, Ed.; Cambridge University Press: Cambridge, UK, 2014; pp. 1199–1266.
10. Patricola, C.; Cook, K. Sub-Saharan Northern African climate at the end of the twenty-first century: Forcing factors and climate change processes. *Clim. Dyn.* **2011**, *37*, 1165–1188. [CrossRef]
11. Oguntunde, P.G.; Abiodun, B.J. The impact of climate change on the Niger River Basin hydroclimatology, West Africa. *Clim. Dyn.* **2013**, *40*, 81–94. [CrossRef]
12. Osuch, M.; Romanowicz, R.; Lawrence, D.; Wong, W. Assessment of the influence of bias correction on meteorological drought projections for Poland. *Hydrol. Earth Syst. Sci. Discuss.* **2015**, *12*, 10331–10377.
13. Pan, T.; Wu, S.; Liu, Y. Relative contributions of land use and climate change to water supply variations over yellow river source area in Tibetan plateau during the past three decades. *PLoS ONE* **2015**, *10*, e0123793. [CrossRef]
14. Zhao, Z.; Liu, G.; Liu, Q.; Huang, C.; Li, H. Studies on the spatiotemporal variability of river water quality and its relationships with soil and precipitation: A case study of the Mun River Basin in Thailand. *Int. J. Environ. Res. Public Health* **2018**, *15*, 2466. [CrossRef]
15. Gogoi, P.P.; Vinoj, V.; Swain, D.; Roberts, G.; Dash, J.; Tripathy, S. Land use and land cover change effect on surface temperature over Eastern India. *Sci. Rep.* **2019**, *9*, 8859. [CrossRef] [PubMed]
16. SP/CNDD. *Le Quatrième Rapport sur L'état de L'environnement au Burkina Faso (REEB IV)*; SP/CNDD: Ouagadougou, Burkina Faso, 2018.

17. Shamir, E.; Megdal, S.B.; Carrillo, C.; Castro, C.L.; Chang, H.-I.; Chief, K.; Corkhill, F.E.; Eden, S.; Georgakakos, K.P.; Nelson, K.M. Climate change and water resources management in the Upper Santa Cruz River, Arizona. *J. Hydrol.* **2015**, *521*, 18–33. [CrossRef]
18. Hartmann, H.; Snow, J.A.; Su, B.; Jiang, T. Seasonal predictions of precipitation in the Aksu-Tarim River basin for improved water resources management. *Glob. Planet. Chang.* **2016**, *147*, 86–96. [CrossRef]
19. Shikangalah, R.N.; Mapani, B. Precipitation variations and shifts over time: Implication on Windhoek city water supply. *Phys. Chem. Earth Parts A/B/C* **2019**, *112*, 103–112. [CrossRef]
20. Rivadeneira Vera, J.F.; Zambrano Mera, Y.E.; Pérez-Martín, M.Á. Adapting water resources systems to climate change in tropical areas: Ecuadorian coast. *Sci. Total Environ.* **2020**, *703*, 135554. [CrossRef]
21. Kaboré, P.N.; Ouédraogo, A.; Sanon, P.Y.; Somé, L. Caractérisation de la vulnérabilité climatique dans la région du Centre-Nord du Burkina Faso entre 1961 et 2015. *Climatologie* **2017**, *14*, 82–95. [CrossRef]
22. Bambara, D.; Compaoré, H.; Bilgo, A. Evolution des températures au Burkina Faso entre 1956 et 2015: Cas de Ouagadougou et de Ouahigouya. *Physio-Géo* **2018**, *12*, 23–41. [CrossRef]
23. Gbohoui, Y.P.; Paturel, J.-E.; Fowe, T.; Mounirou, L.A.; Yonaba, R.; Karambiri, H.; Yacouba, H. Impacts of climate and environmental changes on water resources: A multi-scale study based on Nakanbé nested watersheds in West African Sahel. *J. Hydrol. Reg. Stud.* **2021**, *35*, 100828. [CrossRef]
24. Tirogo, J.; Jost, A.; Biaou, A.; Valdes-Lao, D.; Koussoubé, Y.; Ribstein, P. Climate Variability and Groundwater Response: A Case Study in Burkina Faso (West Africa). *Water* **2016**, *8*, 171. [CrossRef]
25. Karambiri, H.; García Galiano, S.; Giraldo, J.; Yacouba, H.; Ibrahim, B.; Barbier, B.; Polcher, J. Assessing the impact of climate variability and climate change on runoff in West Africa: The case of Senegal and Nakambe River basins. *Atmos. Sci. Lett.* **2011**, *12*, 109–115. [CrossRef]
26. Ibrahim, B. Caractérisation des Saisons de Pluies au Burkina Faso dans un Contexte de Changement Climatique et Evaluation des Impacts Hydrologiques sur le Bassin du Nakanbé. Ph.D. Thesis, Université Pierre et Marie Curie-Paris VI, Paris, France, 2012.
27. MECV. *Programme d'action National d'adaptation à la Variabilité et aux Changements Climatiques PANA Burkina Faso*; SP/CNDD: Ouagadougou, Burkina Faso, 2007.
28. Moser, L.; Voigt, S.; Schoepfer, E.; Palmer, S. Multitemporal Wetland Monitoring in Sub-Saharan West-Africa Using Medium Resolution Optical Satellite Data. *IEEE J. Sel. Top. Appl. Earth Obs. Remote Sens.* **2014**, *7*, 3402–3415. [CrossRef]
29. AEN. *Évaluation des Options de Développement des Ressources en eau et Parti D'aménagement et de Gestion Retenu*; AEN: Ouagadougou, Burkina Faso, 2018.
30. DGRE. *Synthèse du Suivi des Ressources en Eau*; DGRE: Ouagadougou, Burkina Faso, 2018.
31. Klein Tank, A.; Zwiers, F.; Zhang, X. *Guidelines on Analysis of Extremes in a Changing Climate in Support of Informed Decisions for Adaptation*; World Meteorological Organization: Geneva, Switzerland, 2009.
32. Shalishe, A.; Bhowmick, A.; Elias, K. Meteorological Drought Monitoring Based on Satellite CHIRPS Product over Gamo Zone, Southern Ethiopia. *Adv. Meteorol.* **2022**, *2022*, 9323263. [CrossRef]
33. Funk, C.; Peterson, P.; Landsfeld, M.; Pedreros, D.; Verdin, J.; Shukla, S.; Husak, G.; Rowland, J.; Harrison, L.; Hoell, A. The climate hazards infrared precipitation with stations—A new environmental record for monitoring extremes. *Sci. Data* **2015**, *2*, 150066. [CrossRef]
34. Dembélé, M.; Zwart, S. Evaluation and comparison of satellite-based rainfall products in Burkina Faso, West Africa. *Int. J. Remote Sens.* **2016**, *37*, 3995–4014. [CrossRef]
35. Funk, C.; Peterson, P.; Peterson, S.; Shukla, S.; Davenport, F.; Michaelsen, J.; Knapp, K.R.; Landsfeld, M.; Husak, G.; Harrison, L. A high-resolution 1983–2016 T max climate data record based on infrared temperatures and stations by the Climate Hazard Center. *J. Clim.* **2019**, *32*, 5639–5658. [CrossRef]
36. Sacré, R.M.; Didi Mouhamed, L.; Kouakou, K.; Adeline, B.; Arona, D.; Houebagnon Saint, J.C.; Koffi Claude, A.K.; Talnan Jean, H.C.; Salomon, O.; Issiaka, S. Using the CHIRPS Dataset to Investigate Historical Changes in Precipitation Extremes in West Africa. *Climate* **2020**, *8*, 84. [CrossRef]
37. Diatta, S.; Diedhiou, C.W.; Dione, D.M.; Sambou, S. Spatial Variation and Trend of Extreme Precipitation in West Africa and Teleconnections with Remote Indices. *Atmosphere* **2020**, *11*, 999. [CrossRef]
38. Quenum, G.M.L.D.; Nkrumah, F.; Klutse, N.A.B.; Sylla, M.B. Spatiotemporal Changes in Temperature and Precipitation in West Africa. Part I: Analysis with the CMIP6 Historical Dataset. *Water* **2021**, *13*, 3506. [CrossRef]
39. Toté, C.; Patricio, D.; Boogaard, H.; Van Der Wijngaart, R.; Tarnavsky, E.; Funk, C. Evaluation of satellite rainfall estimates for drought and flood monitoring in Mozambique. *Remote Sens.* **2015**, *7*, 1758–1776. [CrossRef]
40. New, M.; Hewitson, B.; Stephenson, D.; Tsiga, A.; Kruger, A.; Manhique, A.; Gomez, B.; Coelho, S.; Masisi, D.; Kululanga, E.; et al. Evidence of trends in daily climate extremes over southern and west Africa. *J. Geophys. Res.* **2006**, *111*, 11. [CrossRef]
41. Mahmood, R.; Jia, S. Spatial and temporal hydro-climatic trends in the transboundary Jhelum River basin. *J. Water Clim. Chang.* **2017**, *8*, 423–440. [CrossRef]
42. Frich, P.; Alexander, L.V.; Della-Marta, P.; Gleason, B.; Haylock, M.; Tank, A.K.; Peterson, T. Observed coherent changes in climatic extremes during the second half of the twentieth century. *Clim. Res.* **2002**, *19*, 193–212. [CrossRef]
43. Zhang, X.; Alexander, L.; Hegerl, G.C.; Jones, P.; Tank, A.K.; Peterson, T.C.; Trewin, B.; Zwiers, F.W. Indices for monitoring changes in extremes based on daily temperature and precipitation data. *Wiley Interdiscip. Rev. Clim. Chang.* **2011**, *2*, 851–870. [CrossRef]

44. Mann, H.B. Nonparametric tests against trend. *Econom. J. Econom. Soc.* **1945**, *13*, 245–259. [CrossRef]
45. Sen, P.K. Estimates of the Regression Coefficient Based on Kendall's Tau. *J. Am. Stat. Assoc.* **1968**, *63*, 1379–1389. [CrossRef]
46. Jaiswal, R.K.; Lohani, A.K.; Tiwari, H.L. Statistical Analysis for Change Detection and Trend Assessment in Climatological Parameters. *Environ. Process.* **2015**, *2*, 729–749. [CrossRef]
47. Wang, Y.; Ma, J.; Xiao, X.; Wang, X.; Dai, S.; Zhao, B. Long-Term Dynamic of Poyang Lake Surface Water: A Mapping Work Based on the Google Earth Engine Cloud Platform. *Remote Sens.* **2019**, *11*, 313. [CrossRef]
48. Siegel, A.F. Robust regression using repeated medians. *Biometrika* **1982**, *69*, 242–244. [CrossRef]
49. Fickas, K.C.; Cohen, W.B.; Yang, Z. Landsat-based monitoring of annual wetland change in the Willamette Valley of Oregon, USA from 1972 to 2012. *Wetl. Ecol. Manag.* **2016**, *24*, 73–92. [CrossRef]
50. Nitze, I.; Grosse, G.; Jones, B.M.; Arp, C.D.; Ulrich, M.; Fedorov, A.; Veremeeva, A. Landsat-based trend analysis of lake dynamics across northern permafrost regions. *Remote Sens.* **2017**, *9*, 640. [CrossRef]
51. Song, X.; Song, S.; Sun, W.; Mu, X.; Wang, S.; Li, J.; Li, Y. Recent changes in extreme precipitation and drought over the Songhua River Basin, China, during 1960–2013. *Atmos. Res.* **2015**, *157*, 137–152. [CrossRef]
52. Tsidu, G.M. Secular spring rainfall variability at local scale over Ethiopia: Trend and associated dynamics. *Theor. Appl. Climatol.* **2017**, *130*, 91–106. [CrossRef]
53. Manzanas, R.; Amekudzi, L.; Preko, K.; Herrera, S.; Gutiérrez, J.M. Precipitation variability and trends in Ghana: An intercomparison of observational and reanalysis products. *Clim. Chang.* **2014**, *124*, 805–819. [CrossRef]
54. Frazier, A.G.; Giambelluca, T.W. Spatial trend analysis of Hawaiian rainfall from 1920 to 2012. *Int. J. Climatol.* **2017**, *37*, 2522–2531. [CrossRef]
55. Pedron, I.T.; Silva Dias, M.A.; de Paula Dias, S.; Carvalho, L.M.; Freitas, E.D. Trends and variability in extremes of precipitation in Curitiba–Southern Brazil. *Int. J. Climatol.* **2017**, *37*, 1250–1264. [CrossRef]
56. Hallouz, F.; Meddi, M.; Mahe, G.; Karahacane, H.; Ali Rahmani, S. Tendance des précipitations et évolution des écoulements dans un cadre de changement climatique: Bassin versant de l'oued Mina en Algérie. *Rev. Des Sci. L'eau J. Water Sci.* **2019**, *32*, 83–114. [CrossRef]
57. Aumond, P.; Can, A.; Mallet, V.; De Coensel, B.; Ribeiro, C.; Botteldooren, D.; Lavandier, C. Kriging-based spatial interpolation from measurements for sound level mapping in urban areas. *J. Acoust. Soc. Am.* **2018**, *143*, 2847–2857. [CrossRef]
58. Li, J.; Heap, A.D. Spatial interpolation methods applied in the environmental sciences: A review. *Environ. Model. Softw.* **2014**, *53*, 173–189. [CrossRef]
59. Guarnier, L.; Barroso, G.F. Spatial and temporal variability of rainfall towards watershed water resources management. *Authorea Prepr.* **2022**.
60. Apaydin, H.; Sonmez, F.K.; Yildirim, Y.E. Spatial interpolation techniques for climate data in the GAP region in Turkey. *Clim. Res.* **2004**, *28*, 31–40. [CrossRef]
61. Lodoun, T.; Giannini, A.; Traoré, P.S.; Somé, L.; Sanon, M.; Vaksmann, M.; Rasolodimby, J.M. Changes in seasonal descriptors of precipitation in Burkina Faso associated with late 20th century drought and recovery in West Africa. *Environ. Dev.* **2013**, *5*, 96–108. [CrossRef]
62. Hoerling, M.; Hurrell, J.; Eischeid, J.; Phillips, A. Detection and attribution of twentieth-century northern and southern African rainfall change. *J. Clim.* **2006**, *19*, 3989–4008. [CrossRef]
63. Funk, C.C.; Rowland, J.; Eilerts, G.; Adoum, A.; White, L. *A Climate Trend Analysis of Burkina Faso*; US Geological Survey: Reston, VA, USA, 2012; pp. 2327–6932.
64. Crawford, A.; Price-Kelly, H.; Terton, A.; Echeverría, D. *Review of Current and Planned Adaptation Action in Burkina Faso*; International Development Research Centre: Ottawa, ON, Canada, 2016. Available online: https://www.authorea.com/doi/full/10.1002/essoar.10503371.1 (accessed on 10 January 2023).
65. Panthou, G.; Lebel, T.; Vischel, T.; Quantin, G.; Sane, Y.; Ba, A.; Ndiaye, O.; Diongue-Niang, A.; Diopkane, M. Rainfall intensification in tropical semi-arid regions: The Sahelian case. *Environ. Res. Lett.* **2018**, *13*, 064013. [CrossRef]
66. Sanogo, S.; Fink, A.H.; Omotosho, J.A.; Ba, A.; Redl, R.; Ermert, V. Spatio-temporal characteristics of the recent rainfall recovery in West Africa. *Int. J. Climatol.* **2015**, *35*, 4589–4605. [CrossRef]
67. Paeth, H.; Fink, A.H.; Pohle, S.; Keis, F.; Mächel, H.; Samimi, C. Meteorological characteristics and potential causes of the 2007 flood in sub-Saharan Africa. *Int. J. Climatol.* **2011**, *31*, 1908–1926. [CrossRef]
68. Barry, A.; Caesar, J.; Klein Tank, A.; Aguilar, E.; McSweeney, C.; Cyrille, A.M.; Nikiema, M.; Narcisse, K.; Sima, F.; Stafford, G. West Africa climate extremes and climate change indices. *Int. J. Climatol.* **2018**, *38*, e921–e938. [CrossRef]
69. IPCC. Summary for Policymakers. In *Global Warming of 1.5 °C*; An IPCC Special Report on the Impacts of Global Warming of 1.5 °C above Pre-Industrial Levels and Related Global Greenhouse Gas Emission Pathways, in the Context of Strengthening the Global Response to the Threat of Climate Change, Sustainable Development, and Efforts to Eradicate Poverty; Masson-Delmotte, V.P., Zhai, H.-O., Pörtner, D., Roberts, J., Skea, P.R., Shukla, A., Pirani, W., Moufouma-Okia, C., Péan, R., Pidcock, S., et al., Eds.; Cambridge University Press: Cambridge, UK; New York, NY, USA, 2018; pp. 3–24. [CrossRef]